The Canadian Mineralogist
Vol. 36, pp. 187-199 (1998)

THE STRUCTURE OF RICHETITE, A RARE LEAD URANYL OXIDE HYDRATE

PETER C. BURNS[1]

Department of Civil Engineering and Geological Sciences, University of Notre Dame, Notre Dame, Indiana 46556-0767, U.S.A.

ABSTRACT

The structure of richetite, approximate formula $M_x Pb_{8.57}[(UO_2)_{18}O_{18}(OH)_{12}]_2(H_2O)_{41}$, $Z = 1$, triclinic, a 20.9391(3), b 12.1000(2), c 16.3450(3) Å, α 103.87(1), β 115.37(1), γ 90.27(1)°, V 3605.2 Å^3, space group $P1$, has been solved by direct methods and refined by full-matrix least-squares techniques to an agreement factor (R) of 8.9% and a goodness-of-fit (S) of 1.79 using 12,383 unique observed reflections ($|F_o| > 4\sigma_F$) collected with Mo$K\alpha$ X-radiation and a CCD (charge-coupled device) area detector. The structure contains 36 unique U^{6+} positions, each of which is part of a near-linear $(U^{6+}O_2)^{2+}$ uranyl ion that is further coordinated by five (O, OH^-) anions, forming pentagonal bipyramids. The uranyl polyhedra share edges to form symmetrically distinct but topologically identical α-U_3O_8-type sheets at $z \approx 0.25$ and $z \approx 0.75$. Although α-U_3O_8-type sheets of uranyl polyhedra occur in several structures, the richetite sheets are unique in their arrangement of OH^- anions. There are 13 partially occupied unique Pb^{2+} sites, two octahedrally coordinated M sites that may contain Fe^{3+} or other cations, and 41 unique H_2O groups in two distinct interlayers at $z \approx 0$ and $z \approx 0.5$. Both the Pb^{2+} and M cations link to uranyl-ion O-atoms from adjacent sheets, and thus provide linkage of the sheets to the interlayer constituents. An extensive network of H bonds provides additional linkage.

Keywords: richetite, uranyl mineral, uranium, structure determination, lead uranyl oxide hydrate.

SOMMAIRE

La structure de la richetite, dont la formule approximative serait $M_x Pb_{8.57}[(UO_2)_{18}O_{18}(OH)_{12}]_2(H_2O)_{41}$, $Z = 1$, triclinique, a 20.9391(3), b 12.1000(2), c 16.3450(3) Å, α 103.87(1), β 115.37(1), γ 90.27(1)°, V 3605.2 Å^3, groupe spatial $P1$, a été résolue par méthode directe et affinée par moindres carrés sur matrice entière jusqu'à un résidu R de 8.9% et un indice de concordance (S) de 1.79 en utilisant 12,383 réflexions uniques observées ($|F_o| > 4\sigma_F$) avec rayonnement Mo$K\alpha$ et un détecteur à aire CCD (à charge couplée). La structure contient 36 positions uniques contenant U^{6+}, chacune d'elles faisant partie d'un ion uranyle $(U^{6+}O_2)^{2+}$ presque linéaire, et de plus coordonné par cinq anions (O, OH^-), pour former des bipyramides pentagonaux. Les polyèdres à uranyle partagent des arêtes pour donner des feuillets de type α-U_3O_8 à $z \approx 0.25$ et $z \approx 0.75$ qui sont distincts en symétrie mais topologiquement identiques. Quoiqu'on trouve des feuillets de type α-U_3O_8 de polyèdres d'uranyle dans plusieurs structures, ceux de la richetite seraient uniques dans leur agencement d'anions OH^-. Il y a 13 sites uniques de Pb^{2+} à occupation partielle, deux sites M à coordinence octaédrique qui pourraient contenir Fe^{3+} ou autres cations, et 41 groupes uniques de H_2O dans deux inter-couches distinctes à des niveaux $z \approx 0$ et $z \approx 0.5$. Les cations Pb^{2+} et M sont liés aux atomes d'oxygène des ions d'uranyle de feuillets adjacents, et assurent donc les liaisons entre les feuillets et les composants logeant entre les feuillets. Un réseau important de liaisons hydrogène fournit des liaisons additionnelles.

(Traduit par la Rédaction)

Mots-clés: richetite, minéral d'uranyle, uranium, détermination de la structure, oxyde d'uranyle de plomb hydraté.

INTRODUCTION

Uranyl minerals are major constituents of the oxidized portions of uranium deposits, where they most commonly occur as the products of alteration of uraninite (Frondel 1958, Finch & Ewing 1992). Despite their importance in environmental issues such as the weathering of radioactive mine tailings and the geological disposal of spent nuclear fuel, uranyl minerals generally are poorly characterized, and there is a lack of systematic work on the structures and stabilities of these minerals, largely because they commonly occur only as complex intergrowths of very small crystals.

Richetite is a rare lead uranyl oxide hydrate that is associated with uraninite and various uranyl minerals in the Shinkolobwe uranium deposits at Shaba, Democratic Republic of Congo. Richetite was originally

[1] *E-mail address*: peter.burns.50@nd.edu

described by Vaes (1947), and a more detailed description was provided by Piret & Deliens (1984), who proposed the formula $PbO•4UO_3•4H_2O$ on the basis of analyses done with an electron microprobe and X-ray photoelectron spectroscopy (XPS). The structure of richetite has never been determined, owing to the small size of the crystals, the high absorption of X rays by the crystals, and the large unit-cell. As part of ongoing work on uranyl minerals (Burns *et al.* 1996, 1997a, b, c, Burns 1997), a structure model has been obtained for richetite using X-ray-diffraction methods and a CCD area detector.

TABLE 1. CRYSTALLOGRAPHIC DATA FOR RICHETITE

a (Å)	20.9391(3)	Crystal size (mm)	0.008x0.20x0.15
b (Å)	12.1000(2)	Radiation	Mo$K\alpha$
c (Å)	16.3450(3)	Total Ref.	23365
α (°)	103.87(1)	Unique Ref.	17810
β (°)	115.37(1)	Unique $\lvert F_o\rvert \geq 4\sigma_F$	12383
γ (°)	90.27(1)	Final R	8.9
V (Å^3)	3605.2	Final S	1.79
		D_{calc}	6.13 g/cm^3
Space group	$P\bar{1}$		
F_{000}	5540		
μ (mm^{-1})	50.6		

Unit-cell contents: $M_{4}Pb_{8.74}[(UO_2)_{18}O_{18}(OH)_{12}]_2(H_2O)_{41}$

$R = \Sigma(|F_o|-|F_c|)/\Sigma|F_o|$

$S = [\Sigma w(|F_o|-|F_c|)^2/(m-n)]^{1/2}$, for m observations and n parameters

EXPERIMENTAL

A specimen containing richetite from the Shinkolobwe mine, Shaba, Democratic Republic of Congo was provided by Mr. William Pinch. The crystals occur as platy aggregates that are seldom larger than 0.2 mm in diameter, each with a pseudohexagonal outline, and with interpenetrating twins common.

X-ray diffraction

A small crystal of richetite, flattened on {001}, was mounted on a Siemens PLATFORM goniometer equipped with a SMART CCD (charge-coupled device) detector, with a crystal-to-detector distance of 5 cm. The SMART CCD detector is a two-dimensional area detector with an active-imaging area 9 cm in diameter. The detector is equipped with a phosphor screen, located immediately behind a beryllium window, to convert the X-ray photons to optical photons that are carried through a fiber-optic taper to the CCD chip. The detector provides improved resolution, sensitivity to weak reflections, and shorter data-collection times than a scintillation counter mounted on a serial diffractometer (Burns 1998).

The data were collected using monochromatic Mo$K\alpha$ X-radiation, a frame width (in ω) of 0.2°, and a 30 s exposure per frame. More than a hemisphere of three-dimensional data was collected, and the data were analyzed to locate peaks for least-squares refinement of the unit-cell dimensions (Table 1). The data were collected for $3° \leq 2\theta \leq 56.5°$, and contained minimum and maximum indices $-24 \leq h \leq 27$, $-16 \leq k \leq 16$, $-21 \leq l \leq 11$. The data were collected in approximately twenty hours, and the intensities of standard reflections showed no significant change during data collection. The data were reduced and filtered for statistical outliers using the Siemens program SAINT. The data were corrected for Lorentz, polarization, and background effects. An empirical absorption-correction was done based upon 438 intense reflections. The crystal was modeled as a (001) plate; reflections with a plate-glancing angle of less than 3° were discarded from the data set, which lowered the $R_{azimuthal}$ of the 438 intense reflections from 10.0 to 2.7%. The plate-glancing angle was selected after trying angles in the range 1 to 5° because it provided the best refinement results. Additional information pertinent to the data is given in Table 1.

Chemical analysis

A cleavage flake of richetite, selected from the same specimen as the crystal used for the X-ray study, was glued to a plexiglass disk and coated with carbon. The crystal was analyzed using a Cameca SX–50 electron microprobe. Energy-dispersion spectra indicated that Pb and U are the only major cations present. Five points were analyzed using the wavelength-dispersion mode, a beam 20 μm in diameter, an excitation voltage of 15 kV, a beam current of 20 nA, and UO_2 and PbTe as standards (Table 2). The structure determination indicated that additional cations may be present in small quantities (see below), so the crystal was analyzed for Al, Ba, Bi, Ca, Co, Cs, Cu, Fe, Mg Mn, Na, Ni, P, S, Sc, Sr, Th, Ti, V, and Zn, but all were found to be below their corresponding detection-limits.

TABLE 2. CHEMICAL COMPOSITION OF RICHETITE (wt. %)

	Point 1	Point 2	Point 3	Point 4	Point 5
UO_3	77.30	77.71	77.83	77.02	77.31
PbO	17.22	16.76	17.04	16.89	17.37

STRUCTURE SOLUTION AND REFINEMENT

Scattering curves for neutral atoms, together with anomalous-dispersion corrections, were taken from *International Tables for X-Ray Crystallography, Vol. IV* (Ibers & Hamilton 1974). The Siemens SHELXTL Version 5 system of programs was used for the determination and refinement of the structure.

Attempts to solve the structure in the space group $P\bar{1}$ were unsuccessful. The structure was solved by direct methods in the space group $P1$. The location

of 36 U atoms was extracted from the solution, and refinement of their positional parameters gave an agreement index (R) of ~25%. A difference-Fourier map calculated at this stage revealed the location of Pb cations and some anions. Additional anions and two additional cation sites (designated M) were gradually located in difference-Fourier maps calculated following least-squares refinement of the improved models. Refinement of the positional parameters for all atoms, the occupancies of the Pb and M sites, the isotropic-displacement parameters for the cations, and an overall isotropic-displacement parameter for all anions gave an agreement index (R) of 10.7%. Refinement of the anisotropic-displacement parameters for the cations, together with two overall isotropic-displacement parameters, one for O^{2-} and OH^-, and one for H_2O, gave an R of 8.9% for 12,383 observed reflections ($|F_O| \geq 4\sigma_F$). The correct absolute orientation of the structure was verified by refinement of the Flack parameter. Several of the uranyl ion U^{6+}–O bond-lengths refined to unreasonably short values (~1.4 Å); all uranyl U^{6+}–O bond-lengths were subsequently restrained to be ~1.8 Å by adding extra weighted observational equations to the least-squares matrix. The imposition of these restraints did not affect the final agreement index. The heavy atoms of the structure were checked for higher symmetry using the program MISSYM (Le Page 1987); no additional symmetry operators were found. Final positional parameters and equivalent isotropic-displacement parameters are given in Table 3, mean interatomic distances of the cation polyhedra are in Table 4, the refined occupancies of the Pb sites are in Table 5, and bond-valence sums at the cation and anion sites are in Table 6. Selected interatomic distances, anisotropic-displacement parameters, and observed and calculated structure-factors are available from the Depository of Unpublished Data, CISTI, National Research Council, Ottawa, Ontario K1A 0S2.

Description of the Structure

Cation polyhedra

The U^{6+} cation is usually present in crystal structures as part of a near-linear $(U^{6+}O_2)^{2+}$ uranyl ion (Ur), with U^{6+}–O bond-lengths of ~1.8 Å (Evans 1963, Burns *et al.* 1997a). The uranyl ion is coordinated by four, five, or six additional anions, located in the equatorial positions of square, pentagonal and hexagonal bipyramids, respectively, such that the O atoms of the uranyl ions (O_{Ur}) form the apices of the bipyramids. The structure of richetite contains 36 symmetrically distinct U^{6+} positions, as shown by bond-valence sums (Table 6) calculated using the bond-valence parameters for U^{6+} proposed by Burns *et al.* (1997a). Each site contains a uranyl ion with $\langle U–O_{Ur}\rangle$ ~1.8 Å, as imposed by soft restraints during the refinement of the structure. All 36 uranyl ions are coordinated by five [O^{2-}, $(OH)^-$] anions, giving $Ur\phi_5$ pentagonal bipyramids (ϕ: unspecified anion). The $\langle U–\phi_{eq}\rangle$ (ϕ_{eq}: equatorial ϕ) bond-lengths range from 2.30 to 2.48 Å, values within the range observed for $Ur\phi_5$ polyhedra in well-refined structures (Burns *et al.* 1997a). Of the 36 U polyhedra, 12 each are $UrO_4(OH)$, $UrO_3(OH)_2$ and $UrO_2(OH)_3$.

The structure of richetite contains 13 symmetrically distinct Pb sites, but site-occupancy refinement indicates that the sites are partially occupied, with occupancies ranging from 0.31(1) to 0.94(1) (Table 5). The $Pb\phi_n$ polyhedra are irregularly shaped and are made up of from seven to nine O_{Ur} anions and H_2O groups, with $\langle Pb–\phi\rangle$ bond-lengths ranging from 2.66 to 2.83 Å (Table 4).

The structure model contains two octahedrally coordinated sites, designated $M(1)$ and $M(2)$, with $\langle M(1)–\phi\rangle$ = 2.07 and $\langle M(2)–\phi\rangle$ = 2.17 Å. Both octahedra are made up of four H_2O groups and two O_{Ur} anions, with the latter in a *trans* arrangement. The polyhedron geometries are consistent with occupancy by Mg^{2+} and Fe^{2+}. The difference-Fourier map, calculated with the $M(1)$ and $M(2)$ sites vacant, indicates that the $M(1)$ site contains substantially more electron density than $M(2)$. A constrained site-occupancy refinement done with the atomic scattering-factors for Fe and Mg gave $M(1)$ = 0.53(5) Mg and 0.47(5) Fe. The predicted mean bond-length, for an octahedron with 0.53 Mg and 0.47 Fe, obtained by summing effective ionic radii (Shannon 1976), is 2.11 Å. The refined site-occupancy for $M(2)$ is 0.30(5) Mg, with the site 70% vacant. If the M sites do contain Fe^{2+} and Mg^{2+}, the crystal contains ~ 0.25 wt.% of both FeO and MgO, which would only be marginally detectable using the electron microprobe. Alternatively, the composition of the crystal selected for the electron-microprobe study may differ slightly from the crystal used for the X-ray study.

Sheets of uranyl polyhedra

Projection of the structure along [010] shows that it is dominated by sheets of uranyl polyhedra, with $Pb\phi_n$ polyhedra, $M\phi_6$ octahedra, and H_2O groups located in the interlayer (Fig. 1). The sheets of uranyl polyhedra at $z \approx 0.25$ and $z \approx 0.75$ are shown projected onto (001) in Figure 2; they are topologically identical to each other, although symmetrically distinct and in different orientations. The corresponding sheet anion-topology, derived using the method of Burns *et al.* (1996), is shown in Figure 3. Richetite is the first lead uranyl oxide hydrate that is known to contain a sheet with this anion topology, although such an arrangement is known from other structures. Burns *et al.* (1996) referred to it as the α-U_3O_8 sheet anion-topology. It can conveniently be described using two distinct chains of polyhedra, the **U** and **P** chains (Miller *et al.* 1996), as shown in Figure 3. The **U** chain is composed of

TABLE 3. ATOMIC PARAMETERS AND ISOTROPIC-DISPLACEMENT PARAMETERS ($x10^4$) FOR RICHETTITE

	x	*y*	*z*	U_{eq}
U(1)	0.1029(2)	0.9383(2)	0.2574(3)	190(10)
U(2)	0.2746(2)	0.4374(3)	0.2824(3)	198(10)
U(3)	0.4449(2)	0.5688(2)	0.2816(3)	97(8)
U(4)	-0.0599(2)	0.4383(3)	0.2653(3)	158(9)
U(5)	-0.2335(2)	0.5781(3)	0.2666(3)	213(9)
U(6)	0.1037(2)	0.5518(3)	0.2542(3)	217(10)
U(7)	0.2542(2)	0.7554(2)	0.2727(3)	90(7)
U(8)	0.5954(2)	0.7629(3)	0.2848(3)	177(9)
U(9)	0.4384(2)	-0.0589(3)	0.2665(3)	162(9)
U(10)	0.4054(2)	0.2443(2)	0.2465(3)	172(9)
U(11)	-0.0931(2)	0.7456(2)	0.2493(3)	146(9)
U(12)	-0.2316(2)	0.9306(3)	0.2728(3)	177(9)
U(13)	0.0976(2)	0.2579(3)	0.2841(3)	176(9)
U(14)	0.6038(2)	0.4389(2)	0.2560(3)	184(10)
U(15)	0.2641(2)	0.0772(3)	0.2661(3)	208(9)
U(16)	-0.2482(2)	0.2520(2)	0.2663(3)	73(7)
U(17)	0.5998(2)	0.0502(3)	0.2457(3)	167(9)
U(18)	-0.0590(2)	0.0678(2)	0.2769(3)	99(8)
U(19)	0.4407(2)	0.2469(3)	0.7556(4)	333(13)
U(20)	0.7549(2)	0.9297(3)	0.7503(3)	218(10)
U(21)	0.9267(2)	0.0746(3)	0.7565(3)	148(9)
U(22)	1.2903(2)	0.7569(3)	0.7862(3)	185(9)
U(23)	1.0950(2)	0.9484(3)	0.7833(3)	171(9)
U(24)	0.4267(2)	-0.0861(3)	0.7555(3)	132(8)
U(25)	0.5995(2)	0.7487(3)	0.7500(3)	126(8)
U(26)	1.1006(2)	0.2430(3)	0.7494(3)	131(8)
U(27)	0.7898(2)	0.2570(3)	0.7852(3)	192(9)
U(28)	1.2631(2)	0.0660(3)	0.7673(3)	171(9)
U(29)	0.9430(2)	0.7501(3)	0.7643(4)	345(12)
U(30)	1.0940(2)	0.5657(3)	0.7765(3)	247(10)
U(31)	0.5917(2)	0.4472(3)	0.7762(3)	122(8)
U(32)	0.5955(2)	0.0658(3)	0.7743(3)	225(10)
U(33)	0.4213(2)	0.5690(3)	0.7460(3)	119(8)
U(34)	1.2507(2)	0.4287(3)	0.7450(3)	216(10)
U(35)	0.9242(2)	0.4132(3)	0.7537(3)	122(8)
U(36)	0.7613(2)	0.5695(3)	0.7670(3)	150(8)
Pb(1)	-0.0303(3)	0.6697(4)	0.5188(4)	341(14)
Pb(2)	0.0744(3)	0.9696(5)	0.5218(5)	264(17)
Pb(3)	0.4636(3)	0.5237(5)	0.5453(5)	219(18)
Pb(4)	0.2337(4)	0.4780(5)	0.4902(5)	272(21)
Pb(5)	0.6172(3)	0.9569(4)	0.0037(4)	385(17)
Pb(6)	0.7119(3)	0.6872(4)	0.0159(5)	410(19)
Pb(7)	1.0800(3)	0.0443(4)	1.0299(4)	164(16)
Pb(8)	0.7266(3)	0.3359(4)	0.5159(4)	270(16)
Pb(9)	-0.0157(3)	0.3152(5)	0.0140(5)	299(19)
Pb(10)	0.6224(3)	0.0312(4)	0.5117(5)	438(18)
Pb(11)	0.1191(7)	0.464(1)	0.009(1)	380(35)
Pb(12)	0.2128(8)	0.187(1)	0.019(1)	463(45)
Pb(13)	0.3066(5)	0.6932(8)	0.5408(8)	413(24)
M(1)	0.349(1)	0.507(2)	0.016(2)	235(38)
M(2)	-0.151(6)	0.013(8)	0.015(9)	235(38)
O(1)	0.147(2)	0.940(3)	0.376(3)	215(9)
O(2)	0.067(2)	0.926(4)	0.131(3)	215(9)
O(3)	0.036(2)	0.074(4)	0.250(4)	215(9)
O(4)	0.203(2)	0.920(4)	0.243(4)	215(9)
O(5)	0.178(3)	0.132(4)	0.296(4)	215(9)
O(6)	0.225(2)	0.379(4)	0.158(3)	215(9)
O(7)	0.325(2)	0.467(3)	0.411(3)	215(9)
O(8)	0.218(3)	0.583(4)	0.286(4)	215(9)
O(9)	0.177(2)	0.393(4)	0.310(4)	215(9)
O(10)	0.318(2)	0.267(4)	0.308(4)	215(9)
O(11)	0.369(3)	0.420(4)	0.260(4)	215(9)
O(12)	0.495(2)	0.565(3)	0.402(3)	215(9)
O(13)	0.398(3)	0.568(4)	0.161(3)	215(9)
O(14)	0.544(2)	0.578(4)	0.263(4)	215(9)
O(15)	-0.111(2)	0.353(3)	0.149(3)	215(9)
O(16)	-0.006(2)	0.520(4)	0.386(3)	215(9)
O(17)	-0.136(3)	0.574(4)	0.251(4)	215(9)
O(18)	0.047(2)	0.393(4)	0.250(4)	215(9)
O(19)	-0.176(2)	0.625(3)	0.396(3)	215(9)
O(20)	-0.186(3)	0.760(4)	0.286(4)	215(9)
O(21)	0.707(3)	0.415(4)	0.237(4)	215(9)
O(22)	0.675(3)	0.628(4)	0.286(4)	215(9)
O(23)	-0.292(2)	0.593(3)	0.144(3)	215(9)
O(24)	0.130(3)	0.624(4)	0.368(3)	215(9)
O(25)	0.079(3)	0.492(4)	0.131(3)	215(9)
O(26)	0.232(2)	0.704(4)	0.154(3)	215(9)
O(27)	0.263(2)	0.798(4)	0.389(3)	215(9)
O(28)	0.635(2)	0.802(3)	0.406(3)	215(9)
O(29)	0.565(3)	0.716(3)	0.162(3)	215(9)
O(30)	0.549(2)	-0.080(4)	0.266(4)	215(9)
O(31)	0.668(3)	0.897(4)	0.284(4)	215(9)
O(32)	0.488(2)	0.027(3)	0.390(3)	215(9)
O(33)	0.387(2)	-0.140(4)	0.151(3)	215(9)
O(34)	0.363(3)	0.071(4)	0.237(4)	215(9)
O(35)	0.355(2)	0.220(4)	0.120(3)	215(9)
O(36)	0.467(2)	0.287(3)	0.368(3)	215(9)
O(37)	-0.145(2)	0.707(4)	0.121(3)	215(9)
O(38)	-0.040(2)	0.785(4)	0.373(3)	215(9)
O(39)	-0.129(2)	0.914(4)	0.252(4)	215(9)
O(40)	-0.274(3)	0.878(4)	0.146(3)	215(9)
O(41)	-0.181(2)	0.974(4)	0.399(3)	215(9)
O(42)	0.706(3)	0.083(4)	0.248(4)	215(9)
O(43)	0.069(3)	0.216(4)	0.159(3)	215(9)
O(44)	0.133(2)	0.294(4)	0.410(3)	215(9)
O(45)	0.648(2)	0.412(4)	0.365(3)	215(9)
O(46)	0.565(2)	0.434(4)	0.131(3)	215(9)
O(47)	0.211(2)	0.083(3)	0.146(3)	215(9)
O(48)	0.321(2)	0.107(4)	0.389(3)	215(9)
O(49)	-0.275(2)	0.207(3)	0.142(3)	215(9)
O(50)	-0.237(2)	0.298(4)	0.385(3)	215(9)
O(51)	0.635(3)	0.129(3)	0.363(3)	215(9)
O(52)	0.563(2)	-0.013(3)	0.122(3)	215(9)
O(53)	-0.109(3)	0.069(4)	0.155(3)	215(9)
O(54)	-0.013(2)	0.065(4)	0.398(3)	215(9)
O(55)	0.418(2)	0.191(4)	0.632(3)	215(9)
O(56)	0.455(2)	0.286(4)	0.878(3)	215(9)
O(57)	0.483(3)	0.417(4)	0.766(4)	215(9)
O(58)	0.476(2)	0.073(4)	0.761(4)	215(9)
O(59)	0.696(2)	0.919(4)	0.628(3)	215(9)
O(60)	0.810(3)	0.934(4)	0.870(3)	215(9)
O(61)	0.649(2)	0.907(4)	0.744(4)	215(9)
O(62)	0.819(3)	0.067(4)	0.742(4)	215(9)
O(63)	0.891(2)	0.022(4)	0.630(3)	215(9)
O(64)	0.975(3)	0.138(4)	0.888(3)	215(9)
O(65)	0.897(2)	0.248(4)	0.743(4)	215(9)
O(66)	0.988(3)	0.928(4)	0.781(5)	215(9)
O(67)	0.039(3)	0.120(4)	0.764(4)	215(9)
O(68)	1.234(2)	0.735(3)	0.663(3)	215(9)
O(69)	1.355(2)	0.793(4)	0.910(3)	215(9)
O(70)	0.318(3)	0.572(4)	0.754(4)	215(9)
O(71)	0.341(3)	0.939(4)	0.792(5)	215(9)
O(72)	0.393(2)	0.742(4)	0.744(4)	215(9)
O(73)	1.069(3)	0.884(4)	0.661(3)	215(9)
O(74)	1.129(2)	1.027(3)	0.907(3)	215(9)
O(75)	0.171(2)	0.092(4)	0.777(4)	215(9)
O(76)	0.371(2)	-0.102(4)	0.631(3)	215(9)
O(77)	0.486(2)	-0.058(3)	0.880(3)	215(9)
O(78)	0.524(3)	-0.125(4)	0.719(4)	215(9)
O(79)	0.571(3)	0.690(4)	0.625(3)	215(9)
O(80)	0.625(3)	0.797(4)	0.875(3)	215(9)
O(81)	0.530(3)	0.610(4)	0.746(4)	215(9)
O(82)	0.666(2)	0.590(4)	0.777(4)	215(9)
O(83)	1.140(2)	0.305(3)	0.873(3)	215(9)
O(84)	1.066(2)	0.170(3)	0.625(3)	215(9)
O(85)	0.143(2)	0.405(4)	0.737(4)	215(9)
O(86)	0.011(2)	0.356(4)	0.715(4)	215(9)
O(87)	0.728(2)	0.222(4)	0.662(3)	215(9)
O(88)	0.854(2)	0.294(4)	0.912(3)	215(9)
O(89)	0.841(3)	0.438(4)	0.803(4)	215(9)
O(90)	1.308(2)	0.143(4)	0.890(3)	215(9)
O(91)	1.214(2)	-0.008(3)	0.646(3)	215(9)
O(92)	0.923(2)	0.708(4)	0.645(3)	215(9)
O(93)	0.951(2)	0.783(3)	0.881(3)	215(9)
O(94)	0.982(3)	0.571(4)	0.766(4)	215(9)
O(95)	1.069(2)	0.572(4)	0.662(3)	215(9)
O(96)	1.123(2)	0.559(4)	0.894(3)	215(9)
O(97)	0.625(3)	0.516(4)	0.901(3)	215(9)
O(98)	0.568(3)	0.378(4)	0.650(3)	215(9)
O(99)	0.624(2)	0.062(4)	0.893(3)	215(9)
O(100)	0.577(2)	0.079(3)	0.657(3)	215(9)
O(101)	0.377(2)	0.509(3)	0.618(3)	215(9)
O(102)	0.467(2)	0.613(4)	0.875(3)	215(9)
O(103)	1.302(3)	0.444(4)	0.868(3)	215(9)
O(104)	1.200(2)	0.404(3)	0.619(3)	215(9)
O(105)	0.979(2)	0.451(3)	0.882(3)	215(9)
O(106)	0.863(2)	0.391(3)	0.624(3)	215(9)

O(107)	0.806(2)	0.636(4)	0.889(3)	215(9)
O(108)	0.719(2)	0.486(3)	0.645(3)	215(9)
OH(1)	-0.014(3)	0.865(4)	0.232(4)	215(9)
OH(2)	0.118(3)	0.734(4)	0.213(4)	215(9)
OH(3)	0.364(2)	0.642(4)	0.327(4)	215(9)
OH(4)	0.478(3)	0.758(4)	0.306(4)	215(9)
OH(5)	0.484(3)	0.369(4)	0.220(5)	215(9)
OH(6)	-0.143(3)	0.390(4)	0.314(4)	215(9)
OH(7)	-0.023(3)	0.263(4)	0.313(4)	215(9)
OH(8)	-0.022(3)	0.594(4)	0.215(4)	215(9)
OH(9)	0.359(2)	0.901(4)	0.313(4)	215(9)
OH(10)	0.477(3)	0.097(4)	0.211(4)	215(9)
OH(11)	-0.143(2)	0.145(4)	0.329(4)	215(9)
OH(12)	0.615(3)	0.234(4)	0.198(4)	215(9)
OH(13)	0.350(2)	0.121(3)	0.718(4)	215(9)
OH(14)	0.350(2)	0.355(4)	0.708(4)	215(9)
OH(15)	0.578(3)	0.261(4)	0.803(4)	215(9)
OH(16)	0.854(2)	0.868(4)	0.722(4)	215(9)
OH(17)	0.716(3)	0.722(4)	0.708(4)	215(9)
OH(18)	0.714(3)	0.131(4)	0.811(4)	215(9)
OH(19)	0.220(3)	0.905(4)	0.834(4)	215(9)
OH(20)	0.212(3)	0.631(4)	0.803(5)	215(9)
OH(21)	0.080(3)	0.771(4)	0.812(4)	215(9)
OH(22)	0.214(3)	0.221(4)	0.707(4)	215(9)
OH(23)	0.710(3)	0.398(4)	0.818(4)	215(9)
OH(24)	0.853(2)	0.621(4)	0.730(4)	215(9)
H_2O(1)	0.389(3)	0.302(5)	0.477(5)	201(16)
H_2O(2)	0.583(2)	0.764(3)	0.016(4)	201(16)
H_2O(3)	0.160(2)	0.120(3)	0.515(4)	201(16)
H_2O(4)	0.106(2)	0.776(3)	0.524(3)	201(16)
H_2O(5)	0.764(2)	0.925(3)	0.019(4)	201(16)
H_2O(6)	0.124(3)	0.531(4)	0.522(4)	201(16)
H_2O(7)	0.287(2)	0.323(3)	0.522(4)	201(16)
H_2O(8)	0.413(2)	0.709(3)	0.544(4)	201(16)
H_2O(9)	0.732(2)	0.982(3)	0.495(4)	201(16)
H_2O(10)	0.782(2)	0.528(3)	0.519(4)	201(16)
H_2O(11)	0.152(2)	0.840(4)	0.014(4)	201(16)
H_2O(12)	0.100(2)	0.269(3)	0.013(4)	201(16)
H_2O(13)	0.577(3)	0.474(4)	0.524(4)	201(16)
H_2O(14)	0.435(2)	0.571(3)	0.011(4)	201(16)
H_2O(15)	-0.089(2)	0.837(3)	0.035(4)	201(16)
H_2O(16)	0.275(2)	0.410(3)	0.026(4)	201(16)
H_2O(17)	0.386(2)	0.332(3)	0.010(4)	201(16)
H_2O(18)	0.291(2)	0.635(3)	0.003(4)	201(16)
H_2O(19)	0.600(2)	0.285(3)	0.523(4)	201(16)
H_2O(20)	0.473(3)	0.171(4)	0.519(4)	201(16)
H_2O(21)	-0.081(2)	0.437(3)	0.495(4)	201(16)
H_2O(22)	0.418(2)	0.025(3)	0.012(4)	201(16)
H_2O(23)	0.278(2)	0.047(4)	0.527(4)	201(16)
H_2O(24)	-0.081(2)	0.525(4)	0.025(4)	201(16)
H_2O(25)	0.768(2)	0.469(3)	0.014(4)	201(16)
H_2O(26)	0.029(2)	0.325(3)	0.508(4)	201(16)
H_2O(27)	0.654(2)	0.647(3)	0.518(4)	201(16)
H_2O(28)	0.411(2)	-0.038(4)	0.513(4)	201(16)
H_2O(29)	0.273(2)	0.948(3)	1.007(4)	201(16)
H_2O(30)	0.958(3)	0.039(4)	0.539(4)	201(16)
H_2O(31)	0.546(2)	0.157(4)	0.036(4)	201(16)
H_2O(32)	0.889(2)	0.800(3)	0.482(4)	201(16)
H_2O(33)	-0.091(2)	0.184(3)	0.514(4)	201(16)
H_2O(34)	0.045(2)	0.663(3)	1.036(4)	201(16)
H_2O(35)	0.481(3)	0.807(5)	0.000(5)	201(16)
H_2O(36)	-0.351(2)	0.346(4)	0.020(4)	201(16)
H_2O(37)	0.531(2)	0.840(3)	0.497(4)	201(16)
H_2O(38)	0.226(3)	0.838(3)	0.517(4)	201(16)
H_2O(39)	0.934(2)	0.102(3)	0.021(4)	201(16)
H_2O(40)	-0.421(3)	0.534(5)	0.024(5)	201(16)
H_2O(41)	-0.185(2)	0.190(3)	0.032(4)	201(16)

TABLE 4. MEAN INTERATOMIC-DISTANCES (Å) FOR RICHETITE

<U(1)-2O_{Ur}>	1.80	<U(2)-2O_{Ur}>	1.81
<U(1)-5ϕ_{eq}>	2.37	<U(2)-5ϕ_{eq}>	2.36
<U(3)-2O_{Ur}>	1.79	<U(4)-2O_{Ur}>	1.79
<U(3)-5ϕ_{eq}>	2.33	<U(4)-5ϕ_{eq}>	2.38
<U(5)-2O_{Ur}>	1.88	<U(6)-2O_{Ur}>	1.74
<U(5)-5ϕ_{eq}>	2.35	<U(6)-5ϕ_{eq}>	2.41
<U(7)-2O_{Ur}>	1.75	<U(8)-2O_{Ur}>	1.74
<U(7)-5ϕ_{eq}>	2.48	<U(8)-5ϕ_{eq}>	2.34
<U(9)-2O_{Ur}>	1.79	<U(10)-2O_{Ur}>	1.79
<U(9)-5ϕ_{eq}>	2.36	<U(10)-5ϕ_{eq}>	2.37
<U(11)-2O_{Ur}>	1.81	<U(12)-2O_{Ur}>	1.80
<U(11)-5ϕ_{eq}>	2.30	<U(12)-5ϕ_{eq}>	2.40
<U(13)-2O_{Ur}>	1.80	<U(14)-2O_{Ur}>	1.78
<U(13)-5ϕ_{eq}>	2.31	<U(14)-5ϕ_{eq}>	2.38
<U(15)-2O_{Ur}>	1.80	<U(16)-2O_{Ur}>	1.79
<U(15)-5ϕ_{eq}>	2.38	<U(16)-5ϕ_{eq}>	2.40
<U(17)-2O_{Ur}>	1.77	<U(18)-2O_{Ur}>	1.81
<U(17)-5ϕ_{eq}>	2.35	<U(18)-5ϕ_{eq}>	2.36
<U(19)-2O_{Ur}>	1.82	<U(20)-2O_{Ur}>	1.80
<U(19)-5ϕ_{eq}>	2.30	<U(20)-5ϕ_{eq}>	2.39
<U(21)-2O_{Ur}>	1.85	<U(22)-2O_{Ur}>	1.81
<U(21)-5ϕ_{eq}>	2.33	<U(22)-5ϕ_{eq}>	2.42
<U(23)-2O_{Ur}>	1.81	<U(24)-2O_{Ur}>	1.82
<U(23)-5ϕ_{eq}>	2.38	<U(24)-5ϕ_{eq}>	2.36
<U(25)-2O_{Ur}>	1.81	<U(26)-2O_{Ur}>	1.80
<U(25)-5ϕ_{eq}>	2.36	<U(26)-5ϕ_{eq}>	2.34
<U(27)-2O_{Ur}>	1.83	<U(28)-2O_{Ur}>	1.79
<U(27)-5ϕ_{eq}>	2.45	<U(28)-5ϕ_{eq}>	2.36
<U(29)-2O_{Ur}>	1.76	<U(30)-2O_{Ur}>	1.76
<U(29)-5ϕ_{eq}>	2.35	<U(30)-5ϕ_{eq}>	2.44
<U(31)-2O_{Ur}>	1.84	<U(32)-2O_{Ur}>	1.81
<U(31)-5ϕ_{eq}>	2.35	<U(32)-5ϕ_{eq}>	2.38
<U(33)-2O_{Ur}>	1.84	<U(34)-2O_{Ur}>	1.80
<U(33)-5ϕ_{eq}>	2.35	<U(34)-5ϕ_{eq}>	2.41
<U(35)-2O_{Ur}>	1.87	<U(36)-2O_{Ur}>	1.79
<U(35)-5ϕ_{eq}>	2.32	<U(36)-5ϕ_{eq}>	2.36
<*Pb*(1)-9ϕ>	2.81	<*Pb*(2)-8ϕ>	2.68
<*Pb*(3)-9ϕ>	2.73	<*Pb*(4)-8ϕ>	2.70
<*Pb*(5)-8ϕ>	2.69	<*Pb*(6)-8ϕ>	2.77
<*Pb*(7)-8ϕ>	2.76	<*Pb*(8)-8ϕ>	2.71
<*Pb*(9)-8ϕ>	2.70	<*Pb*(10)-9ϕ>	2.83
<*Pb*(11)-7ϕ>	2.66	<*Pb*(12)-8ϕ>	2.76
<*Pb*(13)-8ϕ>	2.75		
<*M*(1)-6ϕ>	2.07	<*M*(2)-6ϕ>	2.17

TABLE 5. REFINED SITE-OCCUPANCIES OF THE Pb SITES FOR RICHETITE

Pb(1)	0.94(1)	*Pb*(2)	0.71(1)	*Pb*(3)	0.62(1)	*Pb*(4)	0.62(1)
Pb(5)	0.90(1)	*Pb*(6)	0.81(1)	*Pb*(7)	0.63(1)	*Pb*(8)	0.76(1)
Pb(9)	0.68(1)	*Pb*(10)	0.92(1)	*Pb*(11)	0.34(1)	*Pb*(12)	0.31(1)
Pb(13)	0.50(1)						

alternating triangles and pentagons that share edges, whereas the **P** chain is composed only of pentagons that share edges (Fig. 3). The chains alternate in the sequence **PUPUPU**... in the sheet anion-topology.

Interlayer constituents

The sheets of uranyl polyhedra in the structure of richetite are linked through a complex network of bonds to interlayer constituents (Fig. 1). The interlayers occur at $z \approx 0$ and $z \approx \frac{1}{2}$ and contain Pb^{2+}, *M* cations, and H_2O groups. The Pb^{2+} and *M* cations bond to H_2O groups within the interlayer, as well as to O_{Ur} anions that extend outward from the sheets of uranyl polyhedra.

TABLE 6. BOND-VALENCE* SUMS (*vu*) AT ATOMIC POSITIONS FOR RICHETITE

U(1)	6.03	*O*(6)	1.76	*O*(62)	2.03	*OH*(10)	1.25
U(2)	6.13	*O*(7)	1.72	*O*(63)	1.58	*OH*(11)	1.13
U(3)	6.27	*O*(8)	2.14	*O*(64)	1.63	*OH*(12)	1.12
U(4)	5.87	*O*(9)	1.88	*O*(65)	2.08	*OH*(13)	1.36
U(5)	5.90	*O*(10)	1.60	*O*(66)	2.08	*OH*(14)	1.27
U(6)	6.20	*O*(11)	2.12	*O*(67)	1.95	*OH*(15)	1.32
U(7)	5.76	*O*(12)	1.71	*O*(68)	1.66	*OH*(16)	1.34
U(8)	6.48	*O*(13)	1.97	*O*(69)	1.54	*OH*(17)	1.26
U(9)	6.10	*O*(14)	2.12	*O*(70)	2.09	*OH*(18)	1.28
U(10)	5.98	*O*(15)	1.85	*O*(71)	2.06	*OH*(19)	1.07
U(11)	6.27	*O*(16)	1.76	*O*(72)	2.05	*OH*(20)	1.30
U(12)	5.88	*O*(17)	2.07	*O*(73)	1.82	*OH*(21)	1.31
U(13)	6.52	*O*(18)	2.26	*O*(74)	1.88	*OH*(22)	1.23
U(14)	6.11	*O*(19)	1.55	*O*(75)	2.08	*OH*(23)	1.14
U(15)	6.18	*O*(20)	1.87	*O*(76)	1.70	*OH*(24)	1.41
U(16)	5.90	*O*(21)	2.03	*O*(77)	1.80	H_2O(1)	0.09
U(17)	6.39	*O*(22)	1.77	*O*(78)	1.69	H_2O(2)	0.40
U(18)	6.02	*O*(23)	1.52	*O*(79)	1.71	H_2O(3)	0.19
U(19)	6.23	*O*(24)	2.05	*O*(80)	1.95	H_2O(4)	0.37
U(20)	5.94	*O*(25)	1.93	*O*(81)	1.92	H_2O(5)	0.20
U(21)	5.97	*O*(26)	1.81	*O*(82)	2.03	H_2O(6)	0.18
U(22)	5.56	*O*(27)	1.79	*O*(83)	1.77	H_2O(7)	0.45
U(23)	5.82	*O*(28)	1.94	*O*(84)	1.72	H_2O(8)	0.60
U(24)	6.31	*O*(29)	1.73	*O*(85)	2.03	H_2O(9)	0.34
U(25)	6.08	*O*(30)	2.33	*O*(86)	1.56	H_2O(10)	0.21
U(26)	6.27	*O*(31)	1.92	*O*(87)	1.76	H_2O(11)	0.07
U(27)	5.34	*O*(32)	1.68	*O*(88)	1.69	H_2O(12)	0.58
U(28)	6.27	*O*(33)	1.81	*O*(89)	1.91	H_2O(13)	0.16
U(29)	6.30	*O*(34)	2.01	*O*(90)	1.60	H_2O(14)	0.36
U(30)	5.91	*O*(35)	1.64	*O*(91)	1.80	H_2O(15)	0.02
U(31)	5.75	*O*(36)	1.68	*O*(92)	2.03	H_2O(16)	0.36
U(32)	5.76	*O*(37)	1.66	*O*(93)	1.67	H_2O(17)	0.18
U(33)	5.92	*O*(38)	1.85	*O*(94)	1.99	H_2O(18)	0.41
U(34)	5.90	*O*(39)	2.09	*O*(95)	1.93	H_2O(19)	0.19
U(35)	6.22	*O*(40)	1.88	*O*(96)	1.82	H_2O(20)	0.00
U(36)	6.21	*O*(41)	1.60	*O*(97)	1.83	H_2O(21)	0.12
Pb(1)	1.73	*O*(42)	2.12	*O*(98)	1.43	H_2O(22)	0.00
Pb(2)	1.85	*O*(43)	1.83	*O*(99)	1.98	H_2O(23)	0.00
Pb(3)	1.83	*O*(44)	1.77	*O*(100)	1.63	H_2O(24)	0.08
Pb(4)	2.03	*O*(45)	2.00	*O*(101)	1.83	H_2O(25)	0.10
Pb(5)	1.89	*O*(46)	1.52	*O*(102)	1.49	H_2O(26)	0.00
Pb(6)	1.46	*O*(47)	1.84	*O*(103)	1.93	H_2O(27)	0.00
Pb(7)	1.50	*O*(48)	1.66	*O*(104)	1.68	H_2O(28)	0.00
Pb(8)	1.77	*O*(49)	1.63	*O*(105)	1.60	H_2O(29)	0.02
Pb(9)	1.82	*O*(50)	1.89	*O*(106)	1.53	H_2O(30)	0.15
Pb(10)	1.50	*O*(51)	1.93	*O*(107)	1.71	H_2O(31)	0.11
Pb(11)	1.83	*O*(52)	1.90	*O*(108)	1.86	H_2O(32)	0.55
Pb(12)	1.73	*O*(53)	1.62	*OH*(1)	1.32	H_2O(33)	0.00
Pb(13)	1.92	*O*(54)	1.81	*OH*(2)	1.19	H_2O(34)	0.04
M(1)	2.65	*O*(55)	1.58	*OH*(3)	1.23	H_2O(35)	0.00
M(2)	2.19	*O*(56)	1.51	*OH*(4)	1.37	H_2O(36)	0.00
O(1)	1.77	*O*(57)	2.13	*OH*(5)	1.22	H_2O(37)	0.11
O(2)	1.71	*O*(58)	1.98	*OH*(6)	1.17	H_2O(38)	0.23
O(3)	2.02	*O*(59)	1.84	*OH*(7)	1.27	H_2O(39)	0.21
O(4)	2.12	*O*(60)	1.74	*OH*(8)	1.25	H_2O(40)	0.00
O(5)	1.85	*O*(61)	2.09	*OH*(9)	1.29	H_2O(41)	0.03

*The bond-valence parameters for U^{6+}–O bonds are from Burns *et al.* (1997a) and for Pb^{2+}–O and Fe^{3+}–O are from Brese & O'Keeffe (1991). Bond-valences from Pb^{2+} and *M* cations upon anion positions have been scaled by a factor equal to the refined site-occupancy of the cation site.

Projections of the interlayer polyhedra onto (001) demonstrate that the arrangement at $z \approx 0$ is much different than that at $z \approx ½$ (Figs. 4, 5).

The interlayer at $z \approx 0$ contains six unique $Pb\phi_n$ polyhedra, both $M\phi_6$ octahedra that occur in the structure, as well as four symmetrically distinct H_2O groups that do not bond to either Pb^{2+} or *M* cations. The interlayer contains discrete heteropolyhedral clusters that consist of six partially occupied $Pb\phi_n$ polyhedra and two partially occupied $M\phi_6$ octahedra, and that involve polymerization of polyhedra by the sharing of both corners and faces.

An enlarged view of the heteropolyhedral cluster at $z \approx 0$ is shown in Figure 6. The $Pb(5)\phi_8$ and $Pb(6)\phi_8$ polyhedra, with refined site-occupancies 0.90(1) and 0.81(1), respectively, share a face to form a $Pb_2\phi_{12}$ dimer, with the Pb^{2+} cations separated by 3.828(7) Å. The $Pb_2\phi_{12}$ dimer is linked by corner-sharing with the $M(2)\phi_6$ octahedron to a group of four $Pb\phi_n$ polyhedra (Fig. 6). The $Pb(7)\phi_8$, $Pb(9)\phi_8$, $Pb(11)\phi_7$ and $Pb(12)\phi_8$ polyhedra have refined site-occupancies 0.63(1), 0.68(1), 0.34(1) and 0.31(1), respectively. The *Pb*(7) to *Pb*(12) and *Pb*(9) to *Pb*(11) interatomic distances are 3.36(2) and 3.38(1) Å, respectively. These distances are shorter than is usual for pairs of Pb^{2+} cations, suggesting that only one site of each pair is occupied on a local scale. The sums of the refined site-occupancies are 0.94 for the *Pb*(7) and *Pb*(12) pair, and 1.02 for the *Pb*(9) and *Pb*(11) pair, which is consistent with only one site of each pair being occupied locally. The *Pb*(7) to *Pb*(9) and *Pb*(11) to *Pb*(12) interatomic distances are 3.854(8) and 3.88(2) Å, respectively, long enough for both sites of each pair to be occupied locally. However, on a local scale, occupancy of *Pb*(7)–*Pb*(11) or *Pb*(9)–*Pb*(12) pairs would maintain the linkage to *M*(1). The H_2O(16) anion bonds to the *Pb*(11) and *Pb*(12) sites, and also provides the attachment point for the $M(1)\phi_6$ octahedron (Fig. 6).

The interlayer at $z \approx ½$ contains seven symmetrically distinct $Pb\phi_n$ polyhedra and an additional six symmetrically distinct H_2O groups that are not bonded to Pb^{2+} cations (Fig. 5). The $Pb(1)\phi_9$ polyhedron, with refined site-occupancy 0.94(1), and the $Pb(2)\phi_8$ polyhedron, with refined site-occupancy 0.71(1), share a face with the Pb^{2+} cations separated by 4.210(7) Å. The $Pb(8)\phi_8$ polyhedron, with refined site-occupancy 0.76(1), and the $Pb(10)\phi_9$ polyhedron, with refined site-occupancy 0.92(1), also share a face to form a dimer. The Pb^{2+} cations in the dimer are separated by 4.246(7) Å.

The $Pb(3)\phi_9$, $Pb(4)\phi_8$ and $Pb(13)\phi_8$ polyhedra share elements, and the refined site-occupancies are 0.62(1), 0.62(1) and 0.50(1), respectively. The *Pb*(3) to *Pb*(4) and *Pb*(3) to *Pb*(13) interatomic distances are 4.508(5) and 3.87(1) Å, respectively, whereas the *Pb*(4) and *Pb*(13) cations are separated by 2.77(1) Å only. Therefore, on a local scale, only a combination of the *Pb*(3) and *Pb*(4) or the *Pb*(3) and *Pb*(13) sites are likely to be occupied together, as significant Pb^{2+}–Pb^{2+} repulsion would occur if both the *Pb*(4) and *Pb*(13) sites were occupied locally.

Formula for Richetite

The structure solution indicates that all 36 symmetrically distinct U positions correspond to U^{6+} (see above). The total Pb^{2+}, obtained by summing

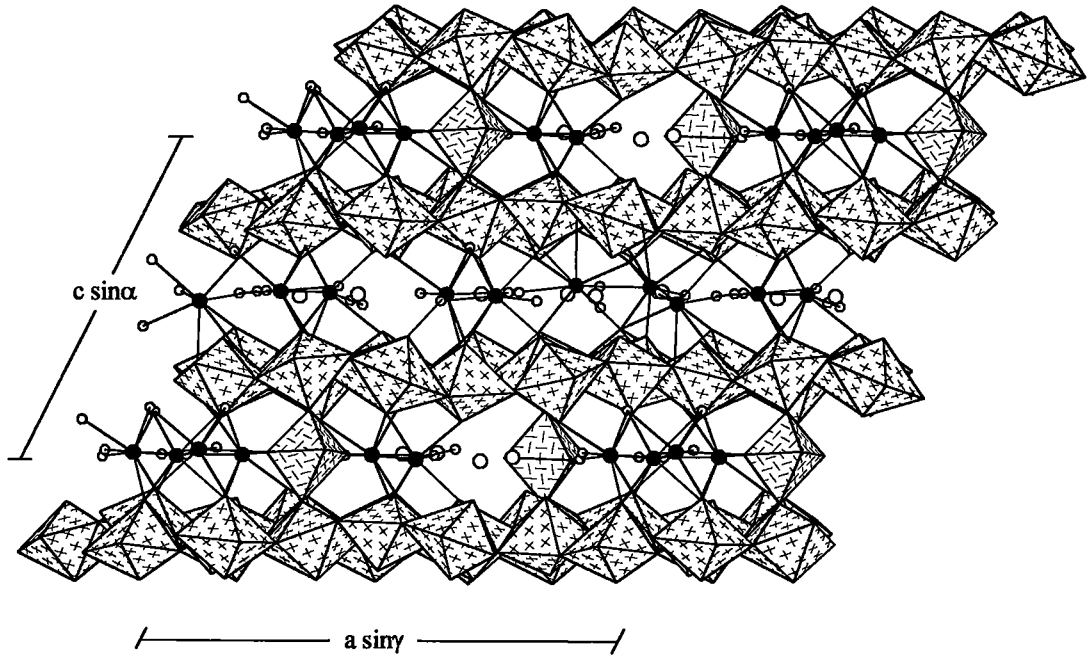

FIG. 1. The structure of richetite projected along [010]. Uranyl polyhedra are shaded with crosses, $M\phi_6$ octahedra are shaded with a herring-bone pattern, Pb^{2+} cations are shown as black circles, O anions and H_2O groups are shown as small and large unshaded circles, respectively.

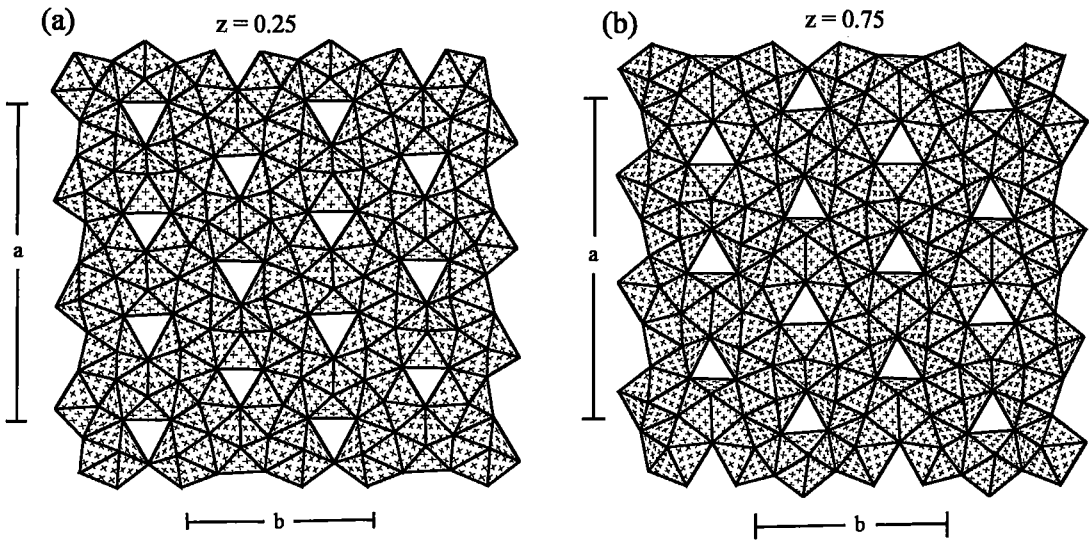

FIG. 2. The sheets of uranyl polyhedra in the richetite structure projected onto (001). Legend as in Figure 1; (a) sheet at $z \approx 0.25$, (b) sheet at $z \approx 0.75$.

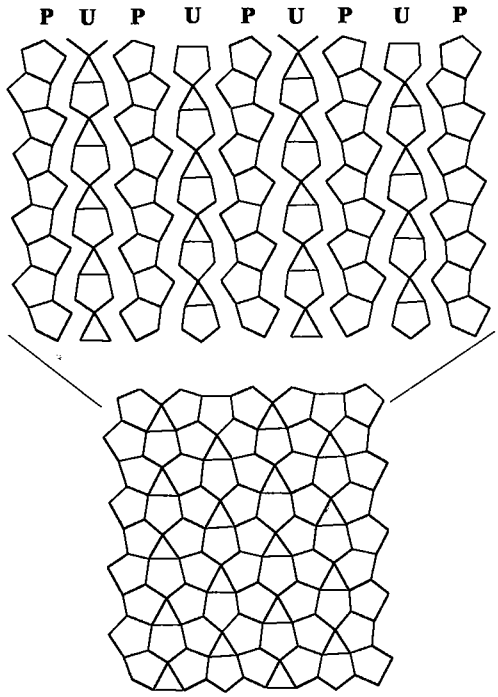

FIG. 3. The richetite sheet anion-topology.

the refined site-occupancies, is 8.74. The polyhedral geometries and electron densities of the two octahedrally coordinated *M* sites are consistent with partial occupancy by Fe^{2+} and Mg^{2+} (see above), and site-occupancy refinement using the atomic scattering-factors for Fe and Mg gave 0.47 Fe^{2+} and 0.83 Mg^{2+}. There are 173 symmetrically distinct anions in the structure, and bond-valence sums (Table 6) indicate these correspond to 108 O^{2-}, 24 $(OH)^-$ and 41 H_2O. The assignment of a few of the anion sites is somewhat ambiguous for the present structure refinement, and it is possible that $(OH)^- \leftrightarrow O^{2-}$ substitution occurs at some of the anion sites.

The formula of the crystal of richetite studied, based upon the structure determination, is $M_xPb_{8.74}[(UO_2)_{18}O_{18}(OH)_{12}]_2(H_2O)_{41}$, where *M* may be Fe^{2+} and Mg^{2+} and, if so, $x = 1.30$. However, the formula has a net charge of –4.1. The chemical analysis of a crystal from the same specimen (Table 2) indicates that the U:Pb ratio is higher than obtained from the structure refinement. The chemical analysis gives a U:Pb ratio of 1:0.282. For a formula with 36 U, the chemical analysis indicates 10.15 Pb^{2+}, which would give a formula with a net charge of –1.2. Further work is required to fully determine the formula of richetite.

COMPARISON TO RELATED SPECIES

Structures with the α-U_3O_8-type sheet

The α-U_3O_8-type sheets of uranyl polyhedra contained in the structure of richetite (Fig. 2) are topologically identical to the sheets that occur in the structures of protasite, $Ba[(UO_2)_3O_3(OH)_2](H_2O)_3$ (Pagoaga *et al.* 1987), billietite, $Ba[(UO_2)_3O_2(OH)_3](H_2O)_4$ (Pagoaga *et al.* 1987), becquerelite, $Ca[(UO_2)_3O_2(OH)_3]_2(H_2O)_8$ (Pagoaga *et al.* 1987), and α-U_3O_8 (Loopstra 1977). The basic anion-topology of the richetite sheet (Fig. 3) does not distinguish between O^{2-} and $(OH)^-$. However, the distribution of O^{2-} and $(OH)^-$ in the sheet is important, as it pertains to the valence of the sheet, as well as to how the sheet connects to interlayer constituents by H bonding. The anion topologies of the sheets in the structure of richetite, with the location of $(OH)^-$ groups indicated as circles, are compared to the anion topologies of the sheets in the structures of protasite, becquerelite and billietite in Figure 7. The distributions of O^{2-} and $(OH)^-$ over the sites in the anion topologies for the richetite sheets at $z \approx 0.25$ and $z \approx 0.75$ in the structure are identical, and all $(OH)^-$ groups are located at the corners of triangles in the anion topology. There are two types of triangles in the richetite sheet anion-topology: type-**A** triangles, which have $(OH)^-$ groups at all corners, and type-**B** triangles, which contain only O^{2-} anions, with twice as many **A** triangles as **B** triangles. Going along any **U** chain in the sheet anion-topology, triangles occur in the sequence **AABAAB**...

In richetite, the sheets have the composition $[(UO_2)_{18}O_{18}(OH)_{12}]^{12-}$, with a ratio of O^{2-} to $(OH)^-$ of 3:2. The sheets in the structure of protasite have the composition $[(UO_2)_3O_3(OH)_2]^{2-}$, with the same ratio of O^{2-} to $(OH)^-$ as in richetite. However, the distribution of $(OH)^-$ groups within the sheet anion-topology of protasite is quite different (Fig. 7). In the sheet anion-topology of protasite, all $(OH)^-$ groups are located at the corners of triangles, such that all triangles in the sheet anion-topology contain two $(OH)^-$ groups. The sheets in the structures of becquerelite and billietite (considering the α-U_3O_8-type sheet only in billietite) have the composition $[(UO_2)_3O_2(OH)_3]^{1-}$, with a ratio of O^{2-} to $(OH)^-$ of 2:3. In the becquerelite and billietite sheet anion-topologies, all $(OH)^-$ groups are located at the corners of triangles, and all triangles contain three $(OH)^-$ groups (Fig. 7). Thus, although the structures of richetite, protasite, becquerelite, and billietite all contain topologically identical sheets, the distribution of $(OH)^-$ groups in the richetite sheet appears to be unique.

Structures of lead uranyl oxide hydrates

Seven lead uranyl oxide hydrate minerals have been described (Finch & Ewing 1992), but the structures are known only for curite, $Pb_3[(UO_2)_8O_8(OH)_6](H_2O)_3$

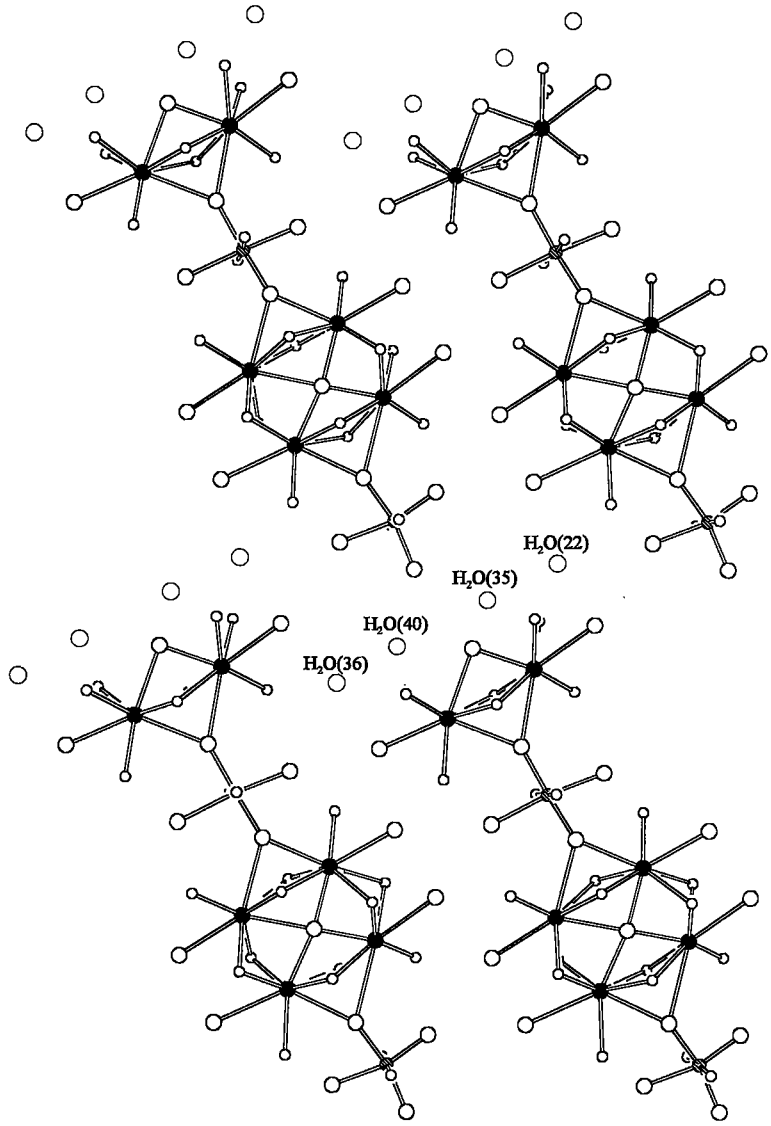

FIG. 4. The interlayer constituents at $z \approx 0$ projected onto (001). Legend as in Figure 1; *M* cations are shown as circles shaded with parallel lines.

(Taylor *et al.* 1981), sayrite, $Pb_2[(UO_2)_5O_6(OH)_2](H_2O)_4$ (Piret *et al.* 1983), fourmarierite, $Pb[(UO_2)_4O_3(OH)_4](H_2O)_4$ (Piret 1985), richetite (this study), and vandendriesscheite, $Pb_{1.57}[(UO_2)_{10}O_6(OH)_{11}](H_2O)_{11}$ (Burns 1997). The structure of each of these minerals is based upon sheets of uranyl polyhedra, with Pb^{2+} cations and H_2O groups located in the interlayers. Richetite is the only lead uranyl oxide hydrate that contains octahedrally coordinated cations in the interlayer.

Each of the lead uranyl oxide hydrate minerals for which structures are known contain different sheets of uranyl polyhedra; the sheets, together with their corresponding sheet anion-topologies, are shown in Figure 8. Of these sheets, only the curite and vandendriesscheite sheets are unique to lead uranyl oxide hydrate structures. Burns (1997) discussed the relationship between the structures and paragenesis of the lead uranyl oxide hydrate minerals.

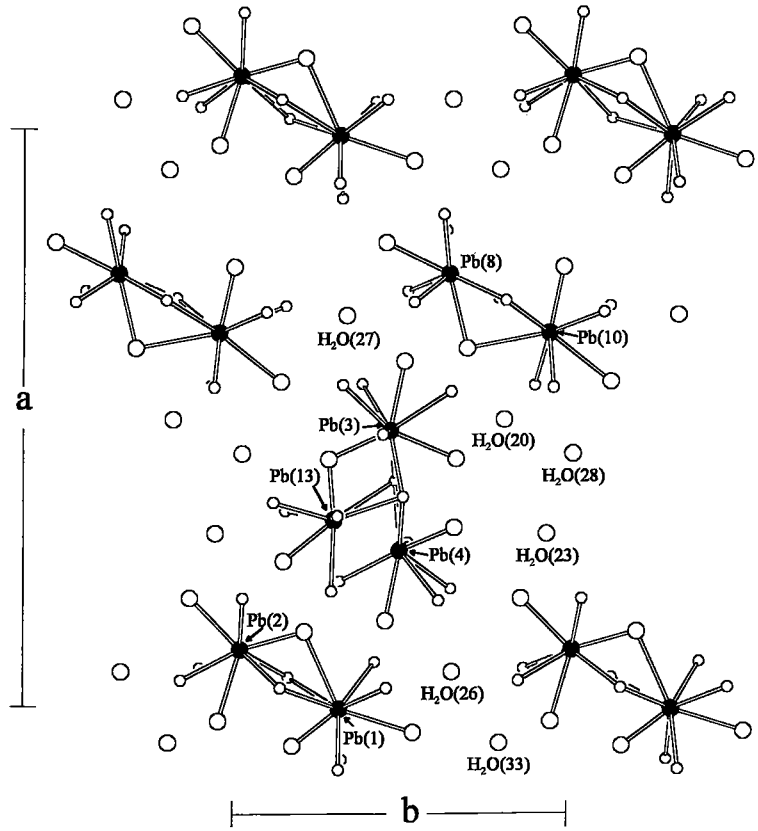

FIG. 5. The interlayer constituents at $z \approx 0.5$ projected onto (001). Legend as in Figures 1 and 4.

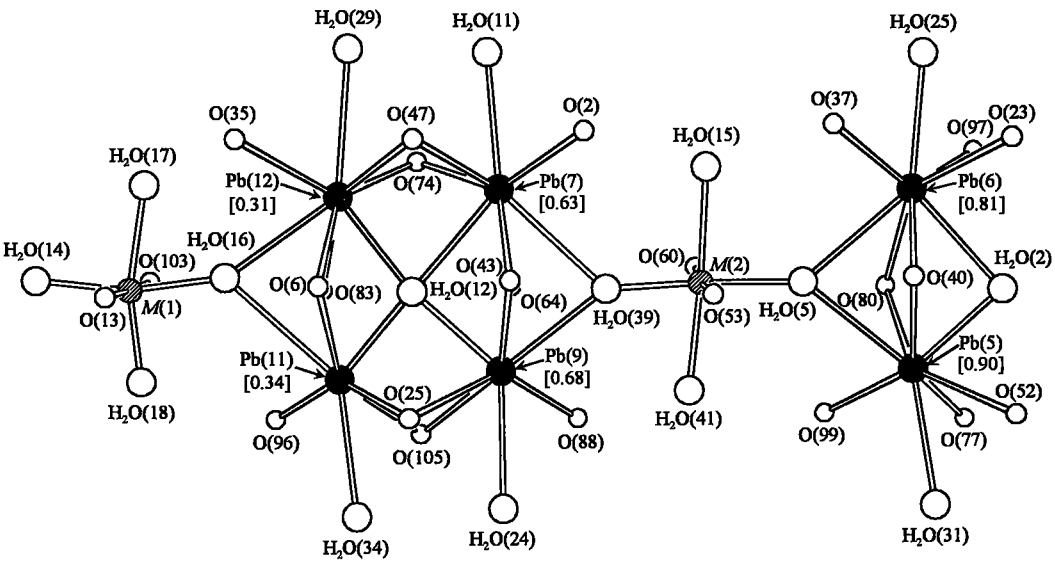

FIG. 6. The heteropolyhedral cluster that occurs in the interlayer at $z \approx 0$ projected onto (001). Legend as in Figures 1 and 4.

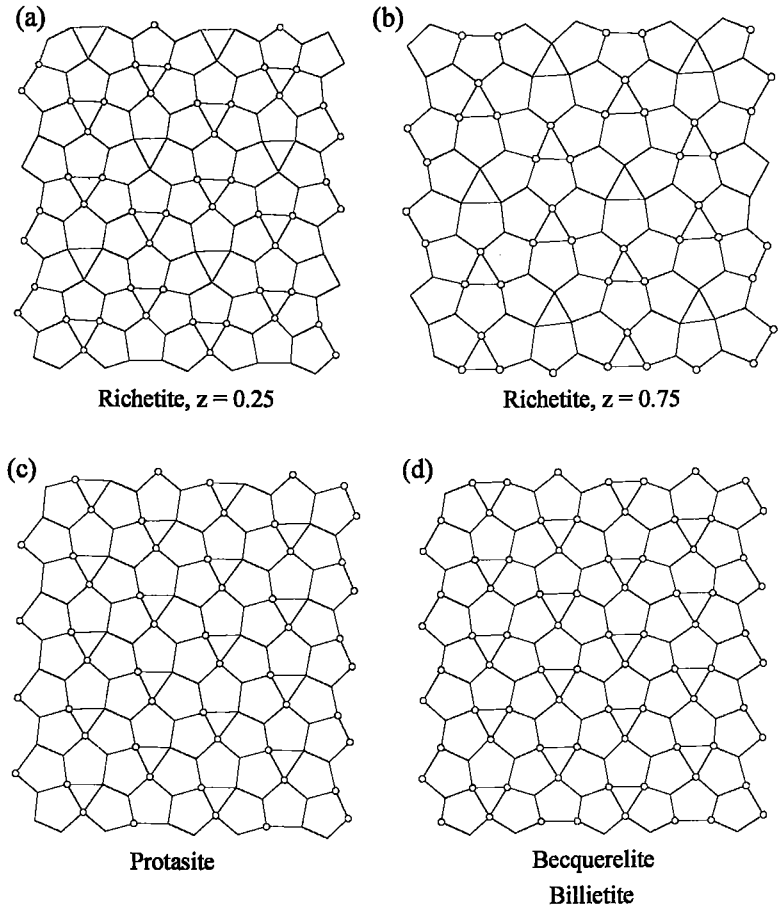

FIG. 7. Sheet anion-topologies with the locations of $(OH)^-$ groups shown by circles for (a) richetite, sheet at $z \approx 0.25$, (b) richetite, sheet at $z \approx 0.75$, (c) protasite, (d) becquerelite and billietite.

ACKNOWLEDGEMENTS

The specimen of richetite was provided by Mr. William Pinch. The electron-microprobe analysis and the single-crystal mount were both provided by Mr. Mark Cooper. This research was supported by the Office of Basic Energy Sciences of the U.S. Department of Energy (Grant No. DE–FG03–93ER45498 to R.C. Ewing). The manuscript was improved following the comments of Mr. Mark Cooper, reviews by Drs. Paul Robinson and John M. Hughes, and editorial work by Robert F. Martin.

REFERENCES

BRESE, N.E. & O'KEEFFE, M. (1991): Bond-valence parameters for solids. *Acta Crystallogr.* **B47**, 192-197.

BURNS, P.C. (1997): A new uranyl oxide hydrate sheet in vandendriesscheite: implications for mineral paragenesis and the corrosion of spent nuclear fuel. *Am. Mineral.* **82**, 1176-1186.

_____ (1998): CCD X-ray area detectors applied to the analysis of mineral structures. *Can. Mineral.* **36** (in press).

_____, EWING, R.C. & HAWTHORNE, F.C. (1997a): The crystal chemistry of hexavalent uranium: polyhedron geometries, bond-valence parameters, and polymerization of polyhedra. *Can. Mineral.* **35**, 1551-1570.

_____, _____ & MILLER, M.L. (1997b): Incorporation mechanisms of actinide elements into the structures of U^{6+} phases formed during the oxidation of spent nuclear fuel. *J. Nucl. Mater.* **245**, 1-9.

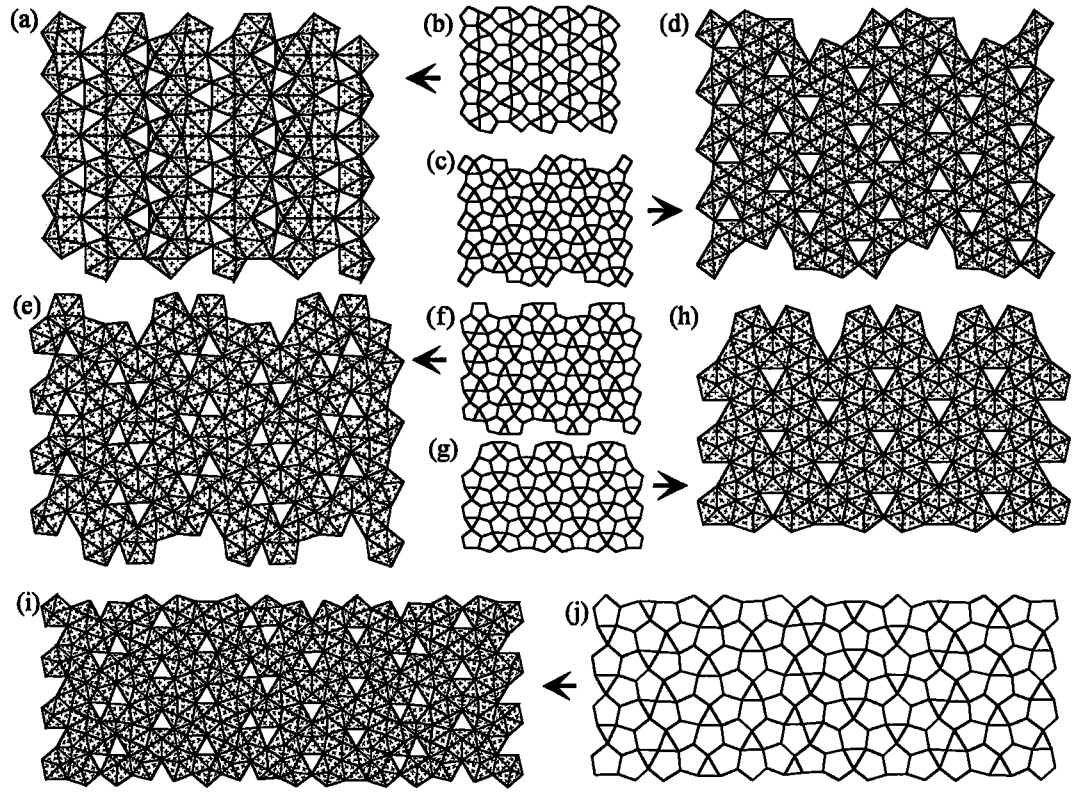

FIG. 8. Polyhedral representations and anion topologies of the sheets that occur in lead uranyl oxide hydrate minerals; (a) curite, (b) curite anion-topology, (c) sayrite anion-topology, (d) sayrite, (e) fourmarietite, (f) fourmarierite anion-topology, (g) richetite anion-topology, (h) richetite, (i) vandendriesscheite, (j) vandendriesscheite anion-topology. The sheet anion-topologies were derived using the method of Burns *et al.* (1996). Uranyl polyhedra are shaded with crosses.

_____, FINCH, R.J., HAWTHORNE, F.C., MILLER, M.L. & EWING, R.C. (1997c): The crystal structure of ianthinite, $[U_2^{4+}(UO_2)_4O_6(OH)_4(H_2O)_4](H_2O)_5$: a possible phase for Pu^{4+} incorporation during the oxidation of spent nuclear fuel. *J. Nucl. Mater.* **249**, 199-206.

_____, MILLER, M.L. & EWING, R.C. (1996): U^{6+} minerals and inorganic phases: a comparison and hierarchy of crystal structures. *Can. Mineral.* **34**, 845-880.

EVANS, H.T., JR. (1963): Uranyl ion coordination. *Science* **141**, 154-157.

FINCH, R.J. & EWING, R.C. (1992): The corrosion of uraninite under oxidizing conditions. *J. Nucl. Mater.* **190**, 133-156.

FRONDEL, C. (1958): Systematic mineralogy of uranium and thorium. *U.S. Geol. Surv., Bull.* **1064**.

IBERS, J.A. & HAMILTON, W.C., eds. (1974): *International Tables for X-ray Crystallography* **IV**. The Kynoch Press, Birmingham, U.K.

LE PAGE, Y. (1987): Computer derivation of the symmetry elements implied in a structure description. *J. Appl. Crystallogr.* **20**, 264-269.

LOOPSTRA, B.O. (1977): On the structure of α-U_3O_8. *J. Inorg. Nucl. Chem.* **B26**, 656-657.

MILLER, M.L., FINCH, R.J., BURNS, P.C. & EWING, R.C. (1996): Description and classification of uranium oxide hydrate sheet anion topologies. *J. Mater. Res.* **11**, 3048-3056.

PAGOAGA, M.K., APPLEMAN, D.E. & STEWART, J.M. (1987): Crystal structures and crystal chemistry of the uranyl oxide hydrates becquerelite, billietite, and protasite. *Am. Mineral.* **72**, 1230-1238.

PIRET, P. (1985): Structure cristalline de la fourmariérite, $Pb(UO_2)_4O_3(OH)_4{\cdot}4H_2O$. *Bull. Minéral.* **108**, 659-665.

_____ & DELIENS, M. (1984): Nouvelles données sur la richetite $PbO.4UO_3.4H_2O$. *Bull. Minéral.* **107**, 581-585.

_____, _____, PIRET-MEUNIER, J. & GERMAIN, G. (1983): La sayrite, $Pb_2[(UO_2)_5O_6(OH)_2]\cdot 4H_2O$, nouveau minéral; propriétés et structure cristalline. *Bull. Minéral.* **106**, 299-304.

SHANNON, R.D. (1976): Revised effective ionic radii and systematic studies of interatomic distances in halides and chalcogenides. *Acta Crystallogr.* **A32**, 751-767.

TAYLOR, J.C., STUART, W.L. & MUMME, I.A. (1981): The crystal structure of curite. *J. Inorg. Nucl. Chem.* **43**, 2419-2423.

VAES, J.F. (1947): Six nouveaux minéraux d'urane provenant de Shinkolobwe (Katanga). *Annales Soc. Géol. Belgique* **70**, B212-B225.

Received September 15, 1997, revised manuscript accepted January 11, 1998.